

Provided for non-commercial research and education use.
Not for reproduction, distribution or commercial use.



This article appeared in a journal published by Elsevier. The attached copy is furnished to the author for internal non-commercial research and education use, including for instruction at the authors institution and sharing with colleagues.

Other uses, including reproduction and distribution, or selling or licensing copies, or posting to personal, institutional or third party websites are prohibited.

In most cases authors are permitted to post their version of the article (e.g. in Word or Tex form) to their personal website or institutional repository. Authors requiring further information regarding Elsevier's archiving and manuscript policies are encouraged to visit:

<http://www.elsevier.com/copyright>



Salophen and salen oxo vanadium complexes as catalysts of sulfides oxidation with H₂O₂: Mechanistic insights

A. Coletti^a, P. Galloni^a, A. Sartorel^b, V. Conte^{a,*}, B. Floris^a

^a Dipartimento di Scienze e Tecnologie Chimiche, Università di Roma Tor Vergata, via della Ricerca Scientifica snc, 00133 Roma, Italy

^b Dipartimento di Scienze Chimiche, Università di Padova, via Marzolo 1, 35131 Padova, Italy

ARTICLE INFO

Article history:

Received 8 November 2011

Received in revised form 5 March 2012

Accepted 8 March 2012

Available online 26 April 2012

Keywords:

Catalytic oxidation

Vanadium complexes

Substituent effect

⁵¹V NMR

DFT calculation

ABSTRACT

The application of V(V) catalysts in oxidation of sulfides with peroxides offers an efficient procedure, that is compatible with different functional groups, and leads to good yields and selectivities. However, the understanding of the factors affecting the reactivity of different catalysts is still far to be complete. An experimental and theoretical study on a series of V(V) complexes containing variously substituted salen and salophen ligands is reported with the aim to correlate the activity of the catalysts with the electronic character of the vanadium center. The results obtained indicate that steric factors play a major role in determining the outcome of the reaction, often overcoming the electronic effects. Theoretical results suggest the intervention in the catalytic cycle of an hydroperoxo vanadium species.

© 2012 Elsevier B.V. All rights reserved.

1. Introduction

Oxidation reactions, and in particular their catalytic versions, often represent key processes to transform bulk chemicals into valuable materials. Millions of tons of such compounds are yearly produced worldwide, and find applications in all areas of chemical industries [1].

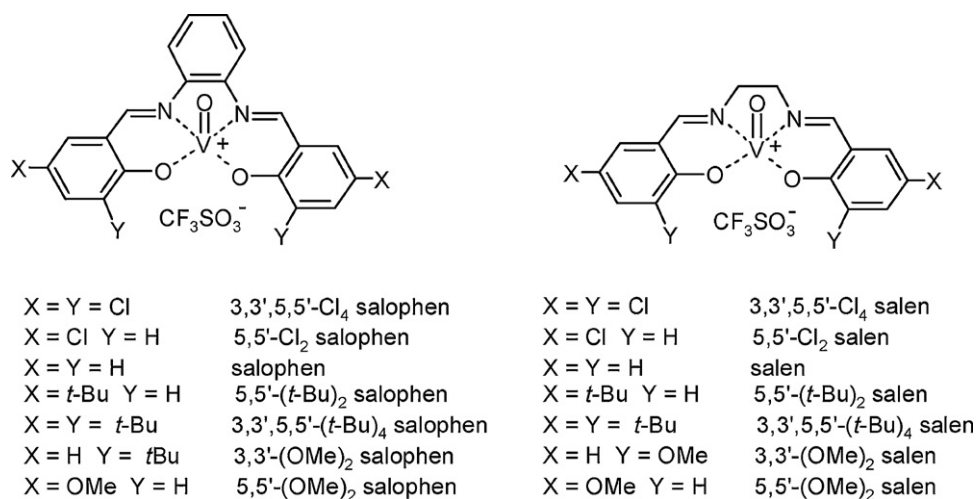
On the basis of economic and environmental reasons [2,3], oxidation processes with H₂O₂ are sustainable processes: first of all H₂O₂ is, besides dioxygen, the most appealing oxidant and the one with the highest “atom efficiency” (47% of active oxygen); in addition, aqueous hydrogen peroxide is readily accessible, safe to use and upon reduction only water is formed [4–7]. Catalytic systems based on different metals have been employed in conjunction with hydrogen peroxide for oxidation reactions [5]. Vanadium catalyzed oxidations with hydrogen peroxide have attracted interest of several research groups because of the interesting properties of this metal in terms of selectivity, reactivity and stereoselectivity. In this perspective, these reactions are also interesting because of the relationship with the reactivity of vanadium-dependent haloperoxidases (VHPO) enzymes, species able to activate hydrogen peroxide for the oxidation of halides, thus producing halogenated compounds, and for stereoselective sulfoxidations of appropriate substrates [8–10].

Peroxo vanadium complexes, formed upon interaction of the metal ion with H₂O₂, depending on the nature of the ligands coordinated to the metal and on the experimental conditions, can act either as electrophilic oxygen transfer reagents or as radical oxidants [11]. Typical electrophilic processes are the oxidation of sulfides and tertiary amines and the epoxidation of allylic alcohol or simple alkenes [11–13]. The oxidation of alcohols and the hydroxylation of aliphatic and aromatic hydrocarbons are examples of homolytic reactivity [5,12,14]. Several review articles have appeared recently on vanadium-catalyzed oxidations [5,15,16].

Additionally, the oxidation of sulfur containing compounds remains an hot research topic both from a synthetic point of view [11,17–19] i.e. the preparation of chiral sulfoxides and of sulfones, as well as considering modern processes for desulfurization of fuels [20]. The removal of sulfur from diesel oil and gasoline is becoming more and more important, not only to protect car exhaust catalysts, but also because of the more strict environment-protecting regulations. Up-to-date, hydrodesulfurization is the method of choice to remove thiols, sulfides, and disulfides, but with this process it is not possible to efficiently remove aromatic sulfur-containing compounds, such as dibenzothiophene and 4,6-dimethyldibenzothiophene. To achieve ultra-deep desulfurization of fuels, oxidation reaction appears to be a promising procedure [21].

This background prompted us to explore the catalytic activity of selected vanadium complexes in oxidation reactions starting from a model sulfide, Ph–S–CH₃, selectively to the corresponding

* Corresponding author. Tel.: +39 0672594014; fax: +39 0672594328.
E-mail address: valeria.conte@uniroma2.it (V. Conte).



Scheme 1. Vanadium(V) salen and salophen complexes.

sulfoxide. The structure of the catalysts used in this study is reported in Scheme 1, they are all oxo vanadium(V) species, ligated with Schiff bases derived from appropriate substituted salicylaldehydes and *o*-phenylenediamine or 1,2-ethanediamine respectively.

Salophen and salen derivatives are considered “privileged ligands” because their easy synthesis by condensation between aldehydes and amines, they also coordinates a wide variety of metals [22]. In addition, stereogenic centers or other elements of chirality can be also introduced. Moreover after appropriate modification heterogeneous catalysts [23] can be prepared.

The variation of the coordination sphere was designed in order to highlight correlation between the electronic distribution on the metal center with the reactivity in oxidation reactions, similar approach has been recently used with vanadium containing strongly related salen and salan complexes [24].

The catalytic activity of some of the species here studied was already recently analyzed in our labs, in the epoxidation of cyclooctene [25]. Quite surprisingly, electron withdrawing groups in the periphery of the salophen ligands reduced the catalytic activity of the vanadium complex toward double bonds. However, this aspect was attributed to faster decomposition of the peroxide. On the other hand, with oxo vanadium salophen complex possessing four *t*-butyl groups in the backbone, the observed reactivity toward cyclooctene was almost zero. In this latter case the prevalence of the steric effect over the electronic one is evident, *i.e.* the bulkiness of the ligand heavily hamper the approach of the substrate to the peroxo complex. Accordingly, in that work [25] no clear cut correlation between the observed reactivity and the coordination environment of the metal center was envisaged.

Moreover, it is to be kept in mind that in vanadium catalyzed oxidations with H₂O₂ two competitive reactions occur: the oxidation of the substrate and the vanadium catalyzed decomposition of hydrogen peroxide [26], for that reason a higher activity of a vanadium complex may simply result in a faster decomposition of H₂O₂.

In this paper we present an experimental and theoretical study, concerning the effects of steric and electronic modification of the ligands on the catalytic activity of salophen and salen oxo vanadium(V) complexes in the oxidation of PhSMe with H₂O₂. This easy to oxidize model substrate has been chosen with the aim to obtain fast and clean oxidation process, good prerequisite for analyzing a class of catalysts which have already shown ambiguous kinetic behavior as function of the substituents present in the salophen or salen scaffolds [25].

2. Procedures

2.1. Experimental

Caution: The uncontrolled heating of large amounts of peroxides must be avoided. Care should be exercised in order to avoid possible explosion.

2.1.1. Instruments

¹H NMR spectra were recorded on a Bruker Avance 300 MHz spectrometer, with CDCl₃, CD₃CN or CD₃COCD₃ as solvents. ⁵¹V NMR spectra were recorded on a Bruker Avance 400 MHz spectrometer, in CD₃CN. HPLC analyses were carried out with a Shimadzu LC-10 ADvp instrument with UV–vis SPD10Avp detector and a Kromasil 100 C18 (250 mm × 4.6 mm, 5 μm) column with V^V complexes or a Metachem Metaphor 50 ODS-2 (250 mm × 4.6 mm, 5 μm) for oxidation reactions. UV–visible spectra were recorded on a SHIMADZU 2450 spectrometer equipped with the UV Probe 2.34 program.

2.1.2. Materials

HPLC-purity grade MeCN was used. Methanol and dichloromethane commercial grade purity were purchased and used as such. Spectroscopic-grade solvents were used for UV–vis spectra. Commercially available aqueous solution of H₂O₂ were used after iodometric titration (10.4 ± 0.2 M H₂O₂ in water).

2.1.3. Synthesis of ligands

The Schiff bases used for the synthesis of the catalysts were prepared by the well known reaction between salicylaldehyde and diamine. Slight experimental variations were introduced with respect to literature methods [27] and the resulting procedure was successfully applied to a number of differently substituted aldehydes.

General procedure: Two equivalents of the appropriate salicylaldehyde were dissolved in the minimum volume of boiling methanol (generally, 20 ml) and added dropwise with one equivalent of diamine (either 1,2-diaminoethane or 1,2-benzenediamine) in 5 ml methanol. The solution was refluxed until all the aldehyde disappeared (TLC analysis) and then cooled to room temperature, thus causing precipitation of the Schiff base, as a yellow solid. The filtered solid was washed with a small amount of methanol, then with diethyl ether and dried. The following Schiff bases were prepared:

Salophen, [1,2-bis-(salicylideneamino)benzene]: yield 95.3%; 5,5'-Cl₂salophen, [1,2-bis-(5-Cl-salicylideneamino)benzene]: yield >99%; 5,5'-(*t*-Bu)₂salophen [1,2-bis-(5-*t*-Bu-salicylideneamino)benzene]: yield 75%; 3,3'-(OMe)₂salophen, [1,2-bis-(3-OMe-salicylideneamino)-benzene]: yield 77%; 5,5'-(OMe)₂salophen, [1,2-bis-(5-OMe-salicylideneamino)-benzene]: yield 79%; 3,3',5,5'-Cl₄salophen [1,2-bis-(3,5-Cl₂salicylideneamino)-benzene]: yield 95%; 3,3',5,5'-(*t*-Bu)₄salophen [1,2-bis-(3,5-di-*t*-Bu-salicylideneamino)benzene]: yield 75%.

Salen, [1,2-bis-(salicylideneamino)ethane]: yield 88%; 5,5'-Cl₂salen, [1,2-bis-(5-Cl-salicylideneamino)ethane]: yield 67%; 5,5'-(*t*-Bu)₂salen, [1,2-bis-(5-*t*-Bu-salicylideneamino)ethane]: yield 91%; 3,3'-(OMe)₂salen, [1,2-bis-(3-methoxy-salicylideneamino)ethane]: yield 92%; 5,5'-(OMe)₂salen, [1,2-bis-(5-OMe-salicylideneamino)ethane]: yield 92%; 3,3',5,5'-Cl₄salen, [1,2-bis-(3,5-Cl₂-salicylideneamino)ethane]: yield 70%; 3,3',5,5'-(*t*-Bu)₄salen, [1,2-bis-(3,5-(*t*-Bu)₂-salicylideneamino)ethane]: yield 72%.

All the compounds gave ¹H NMR and UV–vis spectra consistent with the structure and with literature data [25,28–30].

2.1.4. Synthesis of V^{IV} complexes

The synthesis of these complexes was accomplished by a procedure slightly different from that reported in the literature [31,32]. A number of the vanadium derivatives used in the literature were tested as precursors, *i.e.* VO(acetylacetonate)₂ [31], vanadyl sulfate di-hydrate [29,33], and V(acetylacetonate)₃ [34]. The best results were obtained with V^{III}(acac)₃, in terms of reproducibility of the reaction and solubility of complexes.

General procedure: The Schiff base was dissolved in 100 ml of boiling methanol, or suspended when scarcely soluble. The equimolar amount of V(acac)₃ was completely dissolved in the minimum volume of MeOH with the help of sonication and added dropwise to the solution (or to the suspension), causing immediate color change from yellow to green. After an overnight stirring in an open vessel at room temperature, the reaction was stopped and the precipitated solid was collected, washed with diethyl ether, and dried. No trace of Schiff base was present. Eventually unreacted V(acac)₃ was washed off with warm acetone.

The following V^{IV}O complexes were prepared, their purity was checked with TLC and HPLC analyses.

SalophenV^{IV}O, yield 73%, UV–vis in MeCN [λ_{\max} , nm (ϵ , M⁻¹ cm⁻¹)] 242 (40,000), 314 (22,000) and 396 (18,000); 5,5'-Cl₂salophenV^{IV}O, yield 78%, UV–vis in MeCN [λ_{\max} , nm (ϵ , M⁻¹ cm⁻¹)] 305 (12,000), 409 (10,700); 5,5'-(*t*-Bu)₂salophenV^{IV}O, yield 82%, UV–vis in MeCN [λ_{\max} , nm (ϵ , M⁻¹ cm⁻¹)] 246 (40,900), 318 (22,700), 409 (15,400); 3,3'-(OMe)₂salophenV^{IV}O, yield 79%, UV–vis in MeCN [λ_{\max} , nm (ϵ , M⁻¹ cm⁻¹)] 221 (42,000), 301 (24,000), 313 (22,000) and 335 (13,000); 5,5'-(OMe)₂salophenV^{IV}O, yield 87%, UV–vis in MeCN [λ_{\max} , nm (ϵ , M⁻¹ cm⁻¹)] 216 (70,000), 243 (41,000), 289 (30,000), 300 (32,000), 337 (26,000) and 434 (9000); 3,3',5,5'-Cl₄salophenV^{IV}O: yield 78%, UV–vis in MeCN [λ_{\max} , nm (ϵ , M⁻¹ cm⁻¹)] 315 (9800), 412 (10,000); 3,3',5,5'-(*t*-Bu)₄salophenV^{IV}O, yield 87%, UV–vis in MeCN [λ_{\max} , nm (ϵ , M⁻¹ cm⁻¹)] 250 (43,300), 327 (25,900), 416 (16,100).

SalenV^{IV}O, yield 89%, UV–vis in MeCN [λ_{\max} , nm (ϵ , M⁻¹ cm⁻¹)] 242 (39,000), 277 (18,000) and 362 (7900); 5,5'-Cl₂salenV^{IV}O, yield 67% UV–vis in MeCN [λ_{\max} , nm] 248 (49,000), 280 sh, 370 (7400); 5,5'-(*t*-Bu)₂salenV^{IV}O, yield 67%, UV–vis in MeCN [λ_{\max} , nm (ϵ , M⁻¹ cm⁻¹)] 246 (56,000), 278 (27,000), 370 (9200); 3,3'-(OMe)₂salenV^{IV}O, yield 93%, UV–vis in MeCN [λ_{\max} , nm (ϵ , M⁻¹ cm⁻¹)] 224 (16,000), 296 (14,000) and 381 (2800); 5,5'-(OMe)₂salenV^{IV}O, yield 86%, UV–vis in MeCN [λ_{\max} , nm (ϵ , M⁻¹ cm⁻¹)] 251 (20,000), 286 sh (8800) and 392 (9000); 3,3',5,5'-Cl₄salenV^{IV}O, yield 70%, UV–vis in MeCN: λ_{\max} = 370 nm (does not dissolve completely); 3,3',5,5'-(*t*-Bu)₄salenV^{IV}O, yield 72%, UV–vis

in CH₂Cl₂ [λ_{\max} , nm (ϵ , M⁻¹ cm⁻¹)] 252 (41,000), 288 (27,000) and 386 (3600). UV–vis spectra are consistent with literature data [35,36].

2.1.5. Synthesis of V^V complexes

The synthesis of these complexes was accomplished by a procedure slightly different from that reported in the literature [34]. For all compounds ¹H NMR spectra are in agreement with the structure (in CD₃CN, aromatic protons resonate in the range 7.1–7.8 ppm, CH=N protons in the range 8.2–8.9 ppm, and –CH₂– protons of salen complexes are around 4.4 ppm). By comparison with authentic samples, TLC and HPLC analyses excluded the presence of V^{IV} species.

General procedure: 200 mg of V^VO complex were dissolved in 30 ml CH₂Cl₂ under stirring. Dioxygen was bubbled 5 min into the solution kept at 0 °C and O₂ atmosphere was ensured with a latex reservoir. 1.2 Equivalents trifluoromethanesulfonic acid were rapidly added, causing darkening of the solution and precipitation of a solid. The reaction mixture was allowed to reach room temperature and stirred until disappearance of V^{IV} species (5 ÷ 20 h). Fine powder of V^V complex was isolated after centrifugation of the reaction mixture (6000 r.p.m.) and decantation of the supernatant solution.

The following V^VO complexes were prepared.

[salophenV^VO] CF₃SO₃, yield 95% UV–vis in MeCN [λ_{\max} , nm (ϵ , M⁻¹ cm⁻¹)] 242 (40,000), 304 (26,000) and 393 (10,000); [5,5'-Cl₂salophenV^VO] CF₃SO₃, yield 98%, UV–vis in MeCN [λ_{\max} , nm (ϵ , M⁻¹ cm⁻¹)] 303 (21,300), 408 (11,200); [5,5'-(*t*-Bu)₂salophenV^VO] CF₃SO₃, yield 35%, UV–vis in MeCN [λ_{\max} , nm (ϵ , M⁻¹ cm⁻¹)] 245 (42,700), 320 (24,300), 407 (14,400); [3,3'-(OMe)₂salophenV^VO] CF₃SO₃, yield 75%, UV–vis in MeCN [λ_{\max} , nm (ϵ , M⁻¹ cm⁻¹)] 220 (64,000), 251 (37,000), 302 (45,000), 310 (42,000), 340 (24,000) and 437 (7200); [5,5'-(OMe)₂salophenV^VO] CF₃SO₃, yield 82%, UV–vis in MeCN [λ_{\max} , nm (ϵ , M⁻¹ cm⁻¹)] 215 (68,000), 242 (41,000), 292 (46000), 300 (45000), 341 (29000) and 435 (4900); [3,3',5,5'-Cl₄salophenV^VO] CF₃SO₃, yield 35%, [λ_{\max} , nm (ϵ , M⁻¹ cm⁻¹)] 313 (19200), 410 (13,700); [3,3',5,5'-(*t*-Bu)₄salophenV^VO] CF₃SO₃, yield 87%, [λ_{\max} , nm (ϵ , M⁻¹ cm⁻¹)] 244 (30,700), 326 (35,300), 416 sh (9300).

[salenV^VO] CF₃SO₃, yield 89%, UV–vis in MeCN [λ_{\max} , nm (ϵ , M⁻¹ cm⁻¹)] 230 (30,000), 296 (14,000) and 347 (7400); [5,5'-Cl₂salenV^VO] CF₃SO₃, yield 67%, UV–vis in MeCN [λ_{\max} , nm (ϵ , M⁻¹ cm⁻¹)] 230 (30,000), 248 (24,000), and 285 (17,000); [5,5'-(*t*-Bu)₂salenV^VO] CF₃SO₃, yield 5%, UV–vis in MeCN [λ_{\max} , nm (ϵ , M⁻¹ cm⁻¹)] 230 (33,400), 250 (27,500) 290 (19,000) and 348 (7500); [3,3'-(OMe)₂salenV^VO] CF₃SO₃, yield 58%, UV–vis in MeCN [λ_{\max} , nm (ϵ , M⁻¹ cm⁻¹)] 281 (12,000), 308 (10,000) and 359 (4200); [5,5'-(OMe)₂salenV^VO] CF₃SO₃, yield 89%, UV–vis in MeCN [λ_{\max} , nm (ϵ , M⁻¹ cm⁻¹)] 288 (12,000) and 391 sh (3000); [3,3',5,5'-Cl₄salenV^VO] CF₃SO₃, yield 66%, UV–vis in MeCN [λ_{\max} , nm (ϵ , M⁻¹ cm⁻¹)] 293 sh (1300) and 345 sh (710); 3,3',5,5'-(*t*-Bu)₄salenV^VO, yield 80%. UV–vis in CH₂Cl₂ [λ_{\max} , nm (ϵ , M⁻¹ cm⁻¹)] 263 (8000), 307 (5600) and 367 sh (2900).

Cyclic voltammetry (CV) characterization reported elsewhere [37] confirmed the electronic effect of the substituents on the vanadium centers in these salenV^{IV}O and salophenV^{IV}O complexes. The higher redox potentials of the salophen complexes with respect to the salen ones indicate that the aromatic ring confers to vanadium a stronger Lewis acidity.

2.1.6. Oxidation of phenyl methyl sulfide with H₂O₂, catalyzed by V^V complexes

The catalytic activity of all the complexes was tested in a probe reaction, *i.e.* oxidation of PhSMe with H₂O₂ in MeCN. The reactions were performed with the same initial concentration of all the

reactant species, at 25 °C in a thermostated vessel. Product analysis was obtained by HPLC, to avoid thermal decomposition of products, adding a known amount of toluene as internal standard and using the response factors obtained by calibration straight lines. Stock solutions of sulfide and toluene in MeCN were used. The latter was periodically checked for the presence of oxidation product that were always absent. Solutions of H₂O₂ and the catalyst were prepared immediately before use.

0.5 ml of PhSMe 0.151 M in MeCN and 0.15 ml of catalyst 2.2×10^{-3} M in the same solvent were added to 5 ml MeCN. 0.5 ml of the resulting solution were taken and diluted to 5 ml in a volumetric flask containing 2 ml of PhMe 1.2×10^{-3} M in MeCN, to measure initial sulfide concentration. The reaction started after addition of 0.18 ml freshly prepared H₂O₂ 0.145 M in MeCN (obtained diluting to 5 ml 70 μ l 10.4 \pm 0.2 M H₂O₂ in water). Samples were taken at selected reaction times (2, 5, 15, and 40 min) and analyzed at the HPLC.

2.2. Calculations

Pseudopotential LACVP was used for the energy optimization without symmetry constraints. Gaussian 03 program was used for geometry optimizations with the continuum solvent model [38]. Geometry optimizations were performed with Density Functional Theory (DFT) calculations using the B3LYP functional with the 6-31G* basis set [39,40]. Geometries were optimized at the B3LYP/LANL2DZ level, including solvent effects with the IEF-PCM method (MeCN).

All the in vacuum quantum-mechanical calculations were carried out by using *Spartan'08* [41].

3. Results and discussion

3.1. Experimental

3.1.1. Reactivity

The complexes prepared and used in this work contained Schiff base ligands possessing various substituents in the periphery of the aromatic scaffold, see Scheme 1.

All salophen and salen molecules have been prepared following literature procedures [27] starting from the appropriately substituted salicylaldehydes and *o*-phenylenediamine or 1,2-ethanediamine respectively. The various ligands have been subsequently used to synthesize all V^{IV} and V^V complexes in very good yields (see Section 2), following slightly modified literature procedures [27,31,32,34] and the species obtained have been identified by comparison of their properties with literature data.

For comparison purposes, the V^{IV} species, obtained in the first step of the synthesis of vanadates derivatives, were also tested as catalysts in the oxidation reactions, and the collected data were comparable to those observed (and discussed below) with V^V complexes. However, the possible incursion of radical reactions, an expected event when V^{IV} derivatives are used as catalysts in reactions with hydrogen peroxide [11], prompted us to examine the reactivity in oxidation reaction with hydrogen peroxide only with the catalysts in their highest oxidation state. In such a way, minimization of the vanadium catalyzed decomposition of H₂O₂ should occur.

The various substituents introduced in the scaffold of the complexes were chosen with the scope to modify the electronic character of the V^V ion. Furthermore, a consistent comparison between the salophen and salen structure should help in divide the electronic from the structural effects, being the former species forced into a simil-planar configuration, while the latter can experience a fluctional behavior [22]. Accordingly,

broader signals were detected in ¹H NMR spectra with salen complexes: *i.e.* signal for CH=N at 9.23 ppm shows a $\Delta\nu_{1/2} = 7$ Hz for [3,3',5,5'-(*t*-Bu)₄salophenV^VO] CF₃SO₃ while for the corresponding [3,3',5,5'-(*t*-Bu)₄salenV^VO] CF₃SO₃ derivative the same CH=N signal at 8.86 ppm shows a $\Delta\nu_{1/2} = 22$ Hz.

The model reaction has been the oxidation with H₂O₂ of PhSMe to the corresponding sulfoxide, in MeCN at room temperature, the ratio H₂O₂: Cat was *ca.* 50:1. A two-fold excess of the substrate with respect to the oxidant was used in order to ensure selectivity toward the sulfoxide and also to keep roughly constant the concentration of the substrate, at least at the beginning of the reaction.

The sulfide consumption and the sulfoxide formation were determined with quantitative HPLC analysis of the reaction mixture, see Section 2 for details. Sulfide consumption and sulfoxide yield, at selected reaction time, were taken as parameters to compare the reactivity of the various catalysts, the two values (see Tables) are equal within the experimental error $\pm 5\%$. The data concerning the results with salophen complexes are collected in Table 1 whilst those related to salen species are in Table 2.

The Tables also contain the $\Sigma\sigma$ [42] which is the arithmetical sum of the σ values for the substituents introduced into the salophen and salen scaffolds. These values are given to sketch out the electronic effect dictated by their presence. For the complexes used, it can be noted that, spanning from a $\Sigma\sigma$ of about +1, due to the presence of four chlorine atoms, to a value of about -0.8, when four *t*-butyl groups are present, a large variation of the electronic character of the metal ion, *i.e.* its Lewis acidity, should be obtained.

Looking at the data collected in the two tables some general comments can be done: the catalytic effect of the salophen and salen oxo vanadium(V) complexes is quite good; the reaction times are short, most of the oxidations are complete in 15 min at room temperature. This last observation indicates that the vanadium catalyzed decomposition of H₂O₂ is not competing with the oxygen transfer reaction.

However (see Fig. 1), no simple correlation can be detected between the $\Sigma\sigma$ and the sulfoxide yields in both salophen and salen series; additionally, no simple comparison can be made in equally substituted couples of salophen and salen derivatives; this behavior being indeed expected on the basis of our previous studies [25].

Therefore, a deeper insight of the results is necessary in order to highlight, for each catalyst, if electronic or steric effects are playing the major role in determining the reactivity.

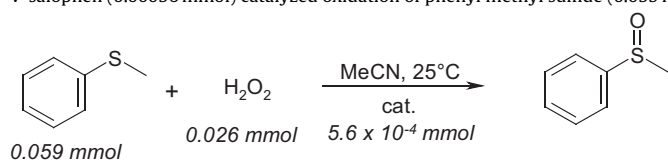
Interestingly, the catalytic activity of substituted salophen complexes, measured as sulfoxide yield at a specific reaction time (left graph), roughly follows the trend of the $\Sigma\sigma$ values with the exception of the 3,3'-(OMe)₂ derivative, this deviation from the expected result will be discussed below. The observed tendency apparently indicates that the reactivity somewhat follows the Lewis acidity character of vanadium, $\Sigma\sigma +0.9$ for 3,3',5,5'-Cl₄-salophen.

On the other hand, with substituted salen derivatives (right graph) no simple correlation can be established between the sulfoxide yields and the $\Sigma\sigma$ values; noteworthy, also in this series the 3,3'-(OMe)₂ derivative shows the highest reactivity. In addition, within this catalysts series high reactivity is observed with 5,5' substituted ligands independently from their inductive effect, whereas for 3,3',5,5'-tetra substituted species the reactivity appears to track the electron density around vanadium.

At this point of the discussion, a better understanding of the results obtained in the reactivity studies can be likely obtained looking also at the classical reaction mechanism [3–6,11] proposed for metal catalyzed sulfides oxidation with peroxides.

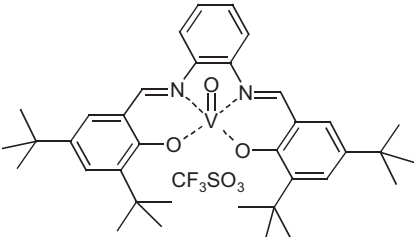
The accepted reaction mechanism for vanadium catalyzed oxidation processes with hydrogen peroxide requires the formation of a peroxide vanadium complex upon coordination of H₂O₂ to the

Table 1
V-salophen (0.00056 mmol) catalyzed oxidation of phenyl methyl sulfide (0.059 mmol) with H₂O₂ (0.026 mmol) in CH₃CN (5.33 ml) at room temperature.



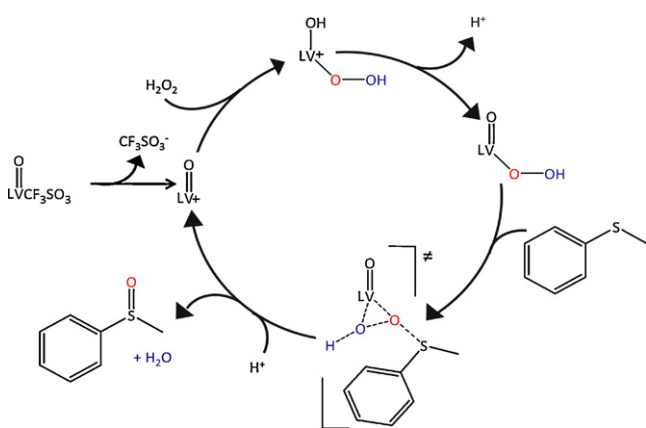
Catalyst	Substituent	t, min	% Sulfide consumed	% Sulfoxide formed ^a	Σσ ^b
	3,3',5,5'-Cl ₄	2	93	94	0.908
		5	93	96	
		15	94	94	
	5,5'-Cl ₂	2	87	92	0.454
		5	91	94	
		15	94	92	
	H	2	54	56	0.000
		5	90	98	
		15	95	100	
	5,5'-(<i>t</i> -Bu) ₂	2	12	1.2	-0.394
		5	14	4.5	
		15	54	53	
	3,3'-(OMe) ₂	2	54	48	-0.536
		5	89	88	
		15	97	96	
	5,5'-(OMe) ₂	2	27	9	-0.536
		5	40	26	
		15	70	62	

Table 1 (Continued)

Catalyst	Substituent	t, min	% Sulfide consumed	% Sulfoxide formed ^a	$\Sigma\sigma^b$
	3,3',5,5'-(<i>t</i> -Bu) ₄	2	18	0	−0.788
		5	24	1.5	
		15	20	6	

^a Sulfide consumption and sulfoxide formation corresponds within the experimental error.

^b $\Sigma\sigma$ is the arithmetical sum of all the σ values [42].



Scheme 2. Proposed catalytic cycle for sulfides oxidation with H₂O₂. L stands for salen or salophen derivatives.

metal center, such intermediate is then the bona fide oxidant of the substrate. For the sake of simplicity, we anticipate here that this active species likely is an hydroperoxo one. The coordination of the oxidant to the Lewis acid metal center activates the oxygen toward the nucleophilic attack of an electron rich substrate, such as the phenyl methyl sulfoxide. In the transition state of the oxidation step, coordination of the second peroxidic oxygen atom to vanadium helps the oxygen transfer to the substrate, subsequent elimination of the sulfoxide and a water molecule regenerates the catalyst precursor (Scheme 2).

With salophen and salen species formation of the peroxidic intermediate can be strongly influenced by the structure of the precursor. In order to consider this structural aspect, energy minimization of the peroxidic species, formed from salophen and salen V^{VO} precursors has been carried out and the outcome for the unsubstituted hydroperoxo oxovanadium complexes (the plausible active oxidant species) is shown in Fig. 2.

For example, salophen ligands force the precursor and the possible peroxy complexes in a *planar* conformation, i.e. the ligand resides on the plane of a simil-tetrahedral shape (see Fig. 2a). On the other hand with salen ligands, together with the *planar* conformation (Fig. 2b) also a *bent* one can be adopted, in which one of the nitrogen of the ligand is trans to the oxo group (see Fig. 2c). It is interesting to note that from theoretical calculation (see following paragraphs), this latter conformation appears to be favorite. The gas phase optimized salenV^V(O)(OOH) and salophenV^V(O)(OOH) structures show that the hydroperoxo group has a different approach to the metal depending on the conformation of the ligand. In particular, when the ligand has a *planar* conformation, like in the case of salophenV^V(O)(OOH), the peroxy group almost adopt the side-on configuration around the metal, thus facilitating the oxygen

transfer to the substrate. On the contrary, when the ligand has a *bent* conformation, like in the case of salenV^V(O)(OOH) (see Fig. 2c) the approach of the second oxygen to the metal is hampered as shown by the longer distance in the calculated structure, thus preventing the stabilization of the transition state.

Summarizing, theoretical calculations suggest that salophen ligands force the hydroperoxovanadium complex in a *planar* conformation that allows the stabilization of the transition state of the oxidation step, resulting in a higher reactivity with respect to salen complexes, where the more stable *bent* conformation can be adopted.

Returning to the experimental data, the higher reactivity of the salophen derivatives, together with the observed relationship of the sulfoxide yields with the Lewis acid character of the vanadium center, appears to be related to the *planar* arrangement of such species which in turn is dictated by the structure of the ligands. On the other hand, with salen derivatives, which can adopt several different conformations because of the mobility of the ligand, the steric hindrance of the substituents combines, in an unpredictable way, with the electronic character of the catalyst.

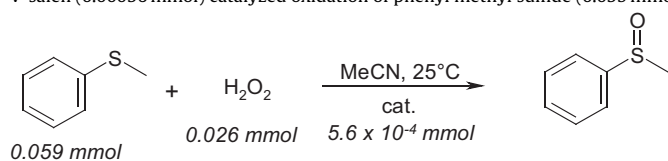
The 3,3' dimethoxy substituted salophen and salen oxovanadium complexes deserve a specific discussion. In fact, the catalytic activity of [3,3'-(OMe)₂salophenV^{VO}][CF₃SO₃] and [3,3'-(OMe)₂salenV^{VO}][CF₃SO₃] is much higher than that of all the other derivatives in the corresponding series (see Fig. 1). This behavior may suggest an easier formation of the metalperoxide species. In that respect, as indicated in Fig. 3, the presence of 3,3'-(OMe)₂ substituents may stabilize the approach of a H₂O₂ molecule to the metal center, through the intervention of an hydrogen bond.

3.1.2. ⁵¹V NMR studies

It is well known that the number and the nature of the peroxo-metal species strongly depends on the reaction conditions, such as the pH value, the ligand and the solvent. Since it is not always possible to obtain peroxovanadium complexes in the solid state, and often their solution structure is different, their structure is often investigated by means of several techniques. For example, ⁵¹V NMR and electrospray ionization mass spectrometry (ESI-MS) or theoretical calculations have been recently used in order to understand their behavior in catalytic cycles [43].

The most common structures of monoperoxovanadium complexes are the side-on cyclic peroxy species, in which both the oxygen atoms are coordinated to vanadium atom, and the hydroperoxo species, in which only one oxygen is covalently linked to the metal center. In this work we have tried to obtain information on the formation in solution of the peroxy derivatives from salophen and/or salen V(V) species, in the presence of different excesses of hydrogen peroxide. ⁵¹V NMR spectra have been acquired for some of the vanadium(V) precursors in acetonitrile and, in all cases, single peaks appeared around −600 ppm. To note,

Table 2
V-salen (0.00056 mmol) catalyzed oxidation of phenyl methyl sulfide (0.059 mmol) with H₂O₂ (0.026 mmol) in CH₃CN (5.33 ml) at room temperature.



Catalyst	Substituents	t, min	% Sulfide consumed	% Sulfoxide formed ^a	Σσ ^b
	3,3',5,5'-Cl ₄	2	12	9	0.908
		5	18	12	
		15	37	35	
	5,5'-Cl ₂	2	76	76	0.454
		5	98	99	
		15	96	98	
	H	2	8	1	0.000
		5	10	4	
		15	18	15	
	5,5'-(<i>t</i> -Bu) ₂	2	92	94	−0.394
		5	88	98	
		15	92	96	
	3,3'-(OMe) ₂	2	>99	>99	−0.536
		5	>99	>99	
		15	>99	>99	
	5,5'-(OMe) ₂	2	34	34	−0.536
		5	62	64	
		15	–	93	
	3,3',5,5'-(<i>t</i> -Bu) ₄	2	92	94	−0.788
		5	88	98	
		15	92	96	

^a Sulfide consumption and sulfoxide formation corresponds within the experimental error.

^b Σσ is the arithmetical sum of all the σ values [42].

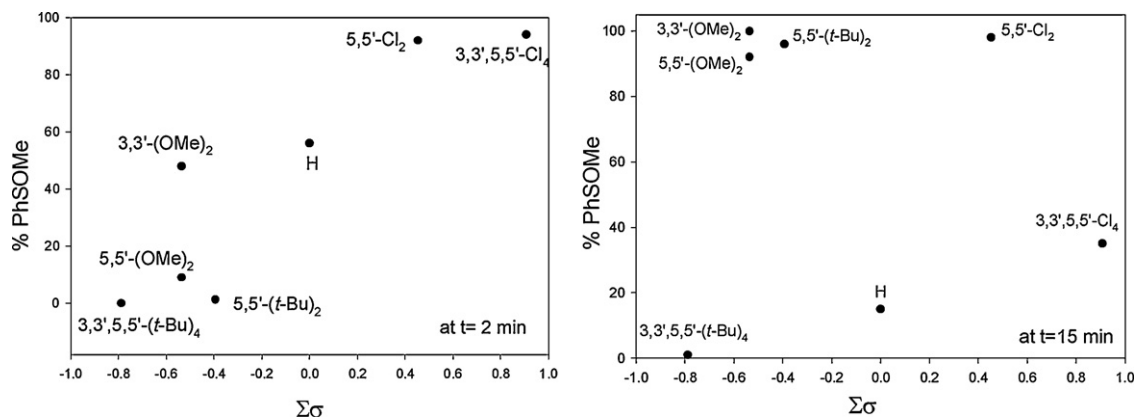


Fig. 1. PhSOMe yields vs. $\Sigma\sigma$ of the ligands. Left: V-salophen catalyzed oxidation of PhSMe with H₂O₂ in CH₃CN at room temperature at 2 min (experimental conditions reported in Table 1). Right: V-salen catalyzed oxidation of PhSMe with H₂O₂ in CH₃CN at room temperature at 15 min (experimental conditions reported in Table 2).

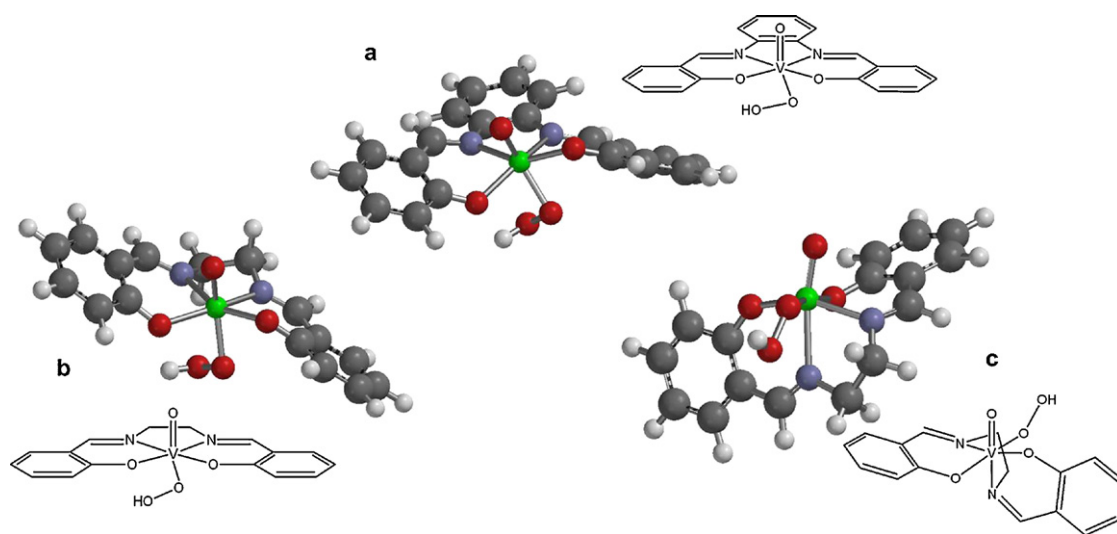


Fig. 2. Gas phase optimized structures of LV^V(O)(OOH) complexes (L=salen or salophen). (a) Planar conformation of salenV^V(O)(OOH). (b) Planar conformation of salophenV^V(O)(OOH). (c) Bent conformation of salenV^V(O)(OOH).

the chemical shifts for salen and salophen species are very similar, despite of the presence of different substituents on the aromatic scaffold.

Upon addition of increasing amounts of H₂O₂ to a solution of [salophenV^VO]CF₃SO₃ or [salenV^VO]CF₃SO₃, the signal of the precursor decreases and, for both complexes, no signals appear having reference to vanadium free ligand species; in general, no other ⁵¹V signals were present in NMR spectra different from that of the

catalyst precursor, over a wide range of chemical shift (as an example, see Fig. 4 for [salenV^VO]CF₃SO₃). Peroxovanadium species usually give signals at high fields [44]; in this case, the absence of any signal may be due to the low solubility of peroxometal species at room temperature. In fact, the formation of a yellow precipitate was observed upon addition of a large excess of H₂O₂ to a solution of salenVO⁺ in acetonitrile.

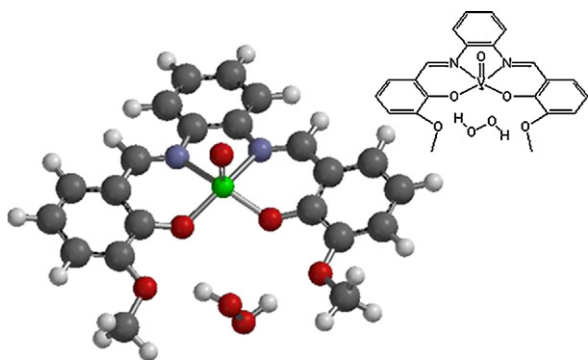


Fig. 3. Plausible formation of a hydrogen bond between an approaching H₂O₂ molecule and the methoxy oxygens in [3,3'-(OMe)₂salophenV^V(O)]CF₃SO₃ complex.

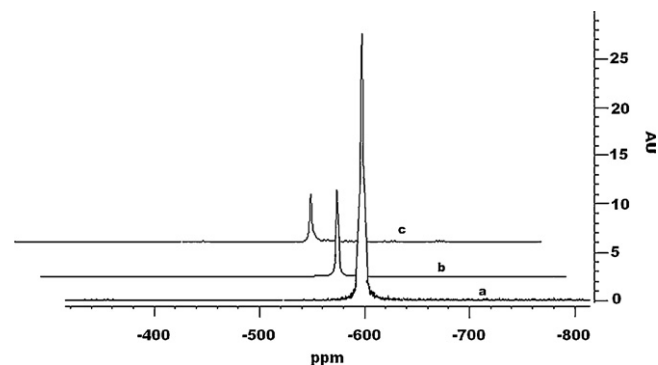


Fig. 4. ⁵¹V NMR spectra of [SalenV^VO]CF₃SO₃ in acetonitrile (1 mM). (a) Initial solution (b) after addition of 2 equivalents of H₂O₂ to the previous solution; (c) after addition of 160 equivalents of H₂O₂ to the initial solution.

Table 3
⁵¹V NMR chemical shifts for different(V) complexes in CH₃CN.

Catalyst	δ ⁵¹ V NMR (ppm)
[salenV ^V O]CF ₃ SO ₃	–597
[5,5'-(Cl) ₂ salenV ^V O]CF ₃ SO ₃	–596
[5,5'-(<i>t</i> -Bu) ₂ salenV ^V O]CF ₃ SO ₃	–584
[salophenV ^V O]CF ₃ SO ₃	–604
[3,3',5,5'-(<i>t</i> -Bu) ₄ salophenV ^V O]CF ₃ SO ₃	–595

The IR spectrum of the yellow precipitate showed no signals in the range of 918–954 cm⁻¹ were the O–O stretching is usually present for side-on monoperoxo vanadium complexes [12], thus supporting the hypothesis that salen and salophen oxovanadium complexes form an end-on hydroperoxidic species in the presence of H₂O₂ (see Section 3 below).

When salenV^VOBr was used as precursor, ⁵¹V NMR spectra in the presence of increasing amount of hydrogen peroxide showed disappearance of the signal at –595 ppm, already after the addition of ten equivalents of H₂O₂. In this conditions no formation of the yellow precipitate was observed. This suggests that the formation of the peroxovanadium species is more favorable when the less tightly coordinated Br⁻ is the counterion in place of CF₃SO₃⁻. In agreement with such observation, when salenV^VOBr was tested as catalyst, a faster decomposition of hydrogen peroxide is observed [5,26].

3.1.3. Theoretical studies

The unclear results obtained with the NMR spectroscopy prompted us to apply DFT theoretical calculations (see Section 2.1 for details) in order to shed more light on the structure of the reactive peroxo complexes formed in solution, when salophen and salen vanadium(V) precursors are used.

Therefore, calculation on relevant species were performed at B3LYP/lanl2dz level, including solvent effects with the IEF-PCM method (acetonitrile). These include vanadium hydroperoxides and η² peroxides, in different protonation forms, and in the presence of a residual oxo or hydroxo ligand (Scheme 3). Frequency calculations were performed in order to confirm that the equilibrium structures were actual minimum energy species (Table 3).

Optimized distances between the vanadium center and the coordinated oxygen of the peroxide moiety fall in the range 1.82–2.05 Å, while oxygen–oxygen distances of the peroxide group are found between 1.46–1.51 Å; both are in good agreement with literature values [45,46]. In general, a decrease of the V–O(O) distance is observed increasing the positive charge of the species [45,46]. When the peroxide is protonated (vanadium hydroperoxides), the protonated oxygen is not located at binding distance from the vanadium center, confirming a monodentate mode of coordination of the O–O group to the metal; differently, when the peroxide moiety is not protonated both oxygen atoms are coordinated to vanadium, in a η² mode [47].

As illustrated in Fig. 2, only planar conformations were considered for salophen complexes, while *bent* and *planar* conformations were explored for all the salenV^V species. To note, as reported in Table 4, some of the salenV^V derivatives are more stable in the *bent* conformation, and in particular the V(O)(OOH) peroxo complex, which is the reasonable active species responsible for oxygen transfer (*vide infra*).

The accepted mechanism, already proposed in the literature, for the formation of peroxidic species resulting from the reaction of vanadium species with hydrogen peroxide [43,45,46] has been used as the base to analyze the energetic path leading to the formation of the peroxo species possibly responsible for oxygen transfer, see Scheme 4.

Table 4
Energetically preferred conformations for salenV^V complexes as derived by DFT calculations.

salenV ^V complex	Bent	Planar	ΔG ^a (kcal mol ⁻¹)
[salenV ^V (OH)(OOH)] ⁺		×	2.3
[salenV ^V O(OOH)]	×		6.7
[salenV ^V (OO)(OH)]		×	1.0
[salenV ^V O(OO)] ⁻	×		14.6

^a Free energy difference between most and less stable conformations for each species.

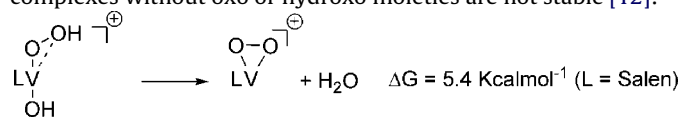
In such scheme the original state of the catalyst was considered to be a LV^VO⁺ species (L stands for salen or salophen ligand) originated from dissociation of LV^VOCF₃SO₃ in solution; addition of H₂O₂ to LV^VO⁺ to form LV^V(OH)(OOH)⁺ species were found to be endothermic processes, with ΔG = +18.1 and +21.4 kcal mol⁻¹ for L = salen and salophen, respectively. For this reason, and considering also the steric hindrance of the ligands around the metal, only the formation of monoperoxo species was taken into account. Moreover, the fact that addition of H₂O₂ are endoergonic processes, suggest that only small amounts of vanadium peroxo complexes form in solution; this result is consistent with ⁵¹V NMR spectra, where no signals different from the one of the precursor have been detected.

Subsequent calculations were aimed at establishing the reactivity of the LV^V(OH)(OOH)⁺ species. A crucial observation is that such intermediates behave as strong acids, by releasing a proton from the hydroxo group to form LV^V(O)(OOH) derivatives (deprotonation step in Scheme 4). This resulted by calculation of the pK_a of the species, by comparison with a reference acid/base couple according to Wang et al. [48]. This procedure avoids direct calculation on H₃O⁺ species, that are subject to relevant solvent effects, difficult to evaluate employing a continuum approximation. In this particular case, the pyridinium/pyridine couple (pK_a = 5.25) was chosen as the reference, in order to maintain the same total charge of the acid/base couple under investigation, LV^V(OH)(OOH)⁺/LV^V(O)(OOH).

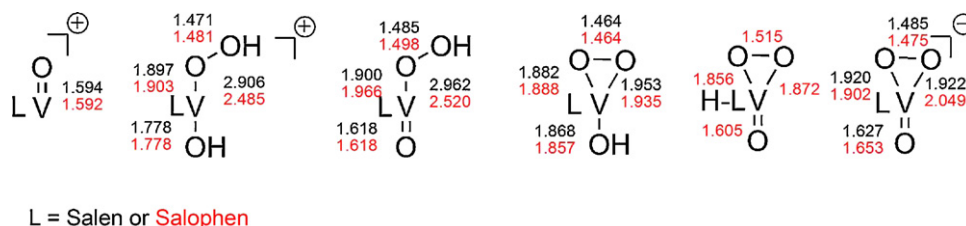
Calculated pK_a for the LV^V(OH)(OOH)⁺/LV^V(O)(OOH) couples were found –6.9 and –4.6 for salen and salophen derivatives, respectively, thus confirming high acid behavior of the hydroxo group coordinated to the vanadium center.

The LV^V(O)(OOH) species were confirmed to be the most probable ones, since possible isomers were observed at higher energy. Indeed, LV^V(OH)(OO) species are higher in energy by 12.5 and 4.1 kcal mol⁻¹ for salen and salophen, respectively, while a H-LV^V(O)(OO) derivative (where the proton is located at the oxygen atom of the L ligand) is 2.2–8.7 kcal mol⁻¹ higher when L = salophen (the same structure with L = salen failed to converge). Protonation of the peroxide species, with no involvement of the oxo group, was recently demonstrated by XANES spectroscopy for a [HheidaV(O)(OO)]⁻ complex (heida = N-(2-hydroxyethyl)iminodiacetic acid) to be the key step to activate the species for oxygen transfer catalysis [49].

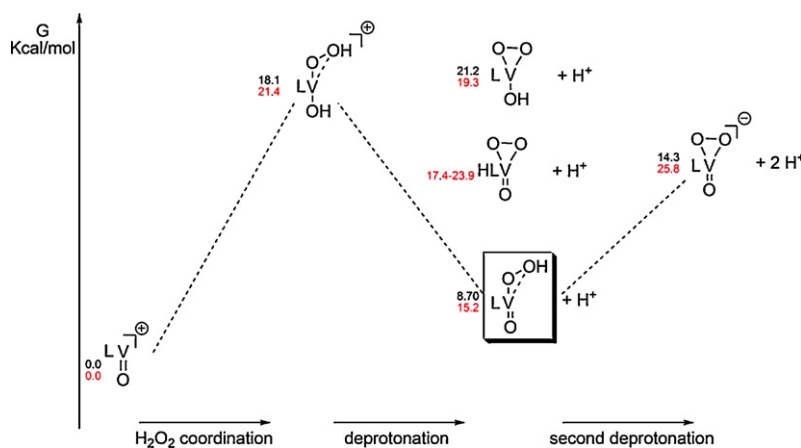
An alternative pathway (not represented in Scheme 4), where water elimination from the LV^V(OH)(OOH)⁺ leads to the formation of a LV^V(OO)⁺ species was found to be endothermic by 5.4 kcal mol⁻¹ in the case of L = salen, confirming that vanadium complexes without oxo or hydroxo moieties are not stable [12]:



Therefore, calculations suggest that a vanadium oxo-hydroperoxo species, LV^V(O)(OOH), is the most plausible intermediate formed upon H₂O₂ addition to vanadium Salen and Salophen complexes, followed by one proton removal. A



Scheme 3. Representation of relevant species considered in DFT calculations, with optimized interatomic distances indicated in black and red for salen and salophen species, respectively. The salen or salophen ligand is represented as “L” for clarity reasons.



Scheme 4. Energies for the formation pathways of various vanadium based peroxy complexes with L = salen (black values) or salophen (red values). The energy of the reactions involving H^+ ions were not directly calculated, but determined indirectly from the calculation of the pK_a of the competent species. (For interpretation of the references to color in this figure legend, the reader is referred to the web version of the article.)

potential, second deprotonation of $L\text{V}^V(\text{O})(\text{OOH})$ to give an anionic $L\text{V}^V(\text{O})(\text{OO})^-$ species was also considered; in these cases calculated pK_a are 4.1 and 7.8 for L = salen and salophen, respectively (in this case acetic acid/acetate has been used as the reference acid/base couple, in order to preserve the charges of the species in the equilibrium process). It is interesting to notice that the calculated pK_a compare reasonably with the values of 5.4–5.9 observed for the vanadium-dependent haloperoxidases enzymes [50,51]. Nevertheless, deprotonated peroxides such as $L\text{V}^V(\text{O})(\text{OO})^-$ are known to be poorly active in oxygen transfer [45,46,49], therefore, even if they could actually be formed in solution according to the pK_a values discussed above, they are not the reasonable catalytically active species in the present system.

Therefore, the presence of the $L\text{V}^V(\text{O})(\text{OOH})$ peroxy complexes in solution is the most reliable scenario. This is in agreement with results found in the literature for similar vanadium complexes with model salan ligands [52], where the oxo hydroperoxy vanadium derivatives appears to be the most favorable active species in alkene epoxidation processes. In such paper, the salan ligand is coordinated to V atom in a bent conformation, in which two O and one N occupy the equatorial positions, while the remaining O is in the axial one; this conformation is consistent with the bent arrangement of the ligand around the vanadium atom that we found for salenVO peroxy complexes.

In the case of salenV(O)(OOH) peroxocomplex, the energies for the *bent* and *planar* conformations of all the 5,5'-substituted derivatives were calculated in the gas phase in order to understand whether the presence of substituents could affect their conformations. The comparison between the two conformations, represented by their energy differences, is reported in Table 5. Interestingly, in all cases the most favorable structure is the *bent* one. For the unsubstituted salen complex, energies in acetonitrile as the model solvent were evaluated, obtaining comparable results.

A final argument concerns the possible oxygen transfer activity of these $L\text{V}(\text{O})(\text{OOH})$ peroxides, namely if they can be the actual species responsible for sulfide oxidation.

As discussed above, the optimized geometries of $L\text{V}(\text{O})(\text{OOH})$ peroxides strongly suggest a monodentate binding of the peroxide to the vanadium center, and it occurs with the non protonated peroxidic oxygen, while the protonated oxygen is not located at binding distance from the vanadium ($\text{V}-\text{O}(\text{H}) = 2.962 \text{ \AA}$ and 2.520 \AA for L = salen and salophen, respectively). This differs from other vanadium hydroperoxy species reported in the literature, where the calculated $\text{V}-\text{O}(\text{H})$ distance is much shorter [45,46] and can be related to the higher steric hindrance of salen and salophen ligands.

As a result, two different scenario can be envisaged: (a) the $L\text{V}(\text{O})(\text{OOH})$ are the actual species for oxygen transfer; indeed the $\text{O}-\text{O} \sigma^*$ orbitals, usually recognized as the one giving the most important contribution in the electrophilic oxidative activity of metal peroxides [53–55], are found at reasonable energy levels for both species (Fig. 5); (b) the $L\text{V}(\text{O})(\text{OOH})$ species are in equilibrium with other forms, where also the second protonated oxygen is coordinated to vanadium, and these latter species are responsible for oxygen transfer:

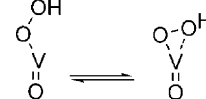


Table 5
Differences of energies for *planar* and *bent* conformations of differently substituted salenV(O)(OOH) species.

salenV(O)(OOH) complex	ΔE (<i>bent-planar</i>) (kcal mol ⁻¹)
[5,5'-(t-Bu) ₂ salenV ^V O(OOH)]	-7.71
[5,5'-(MeO) ₂ salenV ^V O(OOH)]	-8.79
[salenV ^V O(OOH)]	-7.46 (-6.7 in CH ₃ CN)
[5,5'-(Cl) ₂ salenV ^V O(OOH)]	-7.84

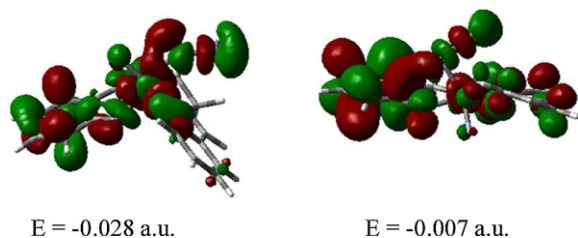


Fig. 5. Representation of the O–O σ^* orbital for SalenV(O)(OOH) (LUMO+6) and SalophenV(O)(OOH) (LUMO+10) species.

Equilibria of this type have already been considered for other V(V) species, where the η^2 coordination of the hydroperoxide was necessary to observe oxygen transfer activity and the free energy of the reaction was influenced by the presence of Lewis bases as coligands [56]. Equilibria of this type are currently under evaluation for salen and salophen derivatives. However, being the distance of the protonated oxygen shorter in the salophen complexes, they may likely establish more easily such equilibrium. On this basis the higher activity of salophen complexes with respect to salen ones could be explained, further support to this is given by their observed higher Lewis acidity as measured with CV experiments [37].

Full mechanistic study, including evaluation of transition states, is in progress and will be reported in a separate communication.

4. Conclusions

The experimental and theoretical results obtained, even though do not allow to draw a decisive picture of the mechanism, let to emphasize that steric factors play a major role in determining the outcome of the reaction, often overcoming the electronic effects. Theoretical results suggest the intervention in the catalytic cycle of an hydroperoxo vanadium species.

Acknowledgements

Research carried out in the framework of COST D40 Action “Innovative Catalysis – New Processes and Selectivities”. Experimental work of S. Ummarino and G. Di Carmine is acknowledged.

Appendix A. Supplementary data

Supplementary data associated with this article can be found, in the online version, at <http://dx.doi.org/10.1016/j.cattod.2012.03.032>.

References

- [1] T. Punniyamurthy, S. Velusamy, J. Ikbali, *Chemical Reviews* 105 (2005) 2329–2363.
- [2] P.T. Anastas, J.T. Warner, *Green Chemistry Theory and Practice*, Oxford University Press, 1998.
- [3] R.A. Sheldon, I. Arends, U. Hanefeld, *Green Chemistry and Catalysis*, Wiley-VCH, Weinheim, Germany, 2007.
- [4] G. Strukul, *Catalytic Oxidation with Hydrogen Peroxide as Oxidant*, Kluwer Academic Publisher, Netherlands, 1992.
- [5] V. Conte, B. Floris, *Inorganica Chimica Acta* 363 (2010) 1935–1946, and references therein.
- [6] V. Conte, A. Coletti, B. Floris, G. Licini, C. Zonta, *Coordination Chemistry Reviews* 255 (2011) 2165–2177, and references therein.
- [7] G. Licini, V. Conte, A. Coletti, M. Mba, C. Zonta, *Coordination Chemistry Reviews* 255 (2011) 2345–2357, and references therein.
- [8] A. Butler, *Coordination Chemistry Reviews* 187 (1999) 17–35, and refs. cited therein.
- [9] V.M. Dembitsky, *Tetrahedron* 59 (2003) 4701–4720.
- [10] A.G.J. Ligtenbarg, R. Hage, B.L. Feringa, *Coordination Chemistry Reviews* 237 (2003) 89–101.
- [11] V. Conte, O. Bortolini, in: Z. Rappoport (Ed.), *The Chemistry of Peroxides – Transition Metal Peroxides Synthesis and Role in Oxidation Reactions*, Wiley Interscience, 2006, pp. 1053–1128.
- [12] V. Conte, B. Floris, *Dalton Transactions* 40 (2011) 1419–1436, and references therein.
- [13] M.L. Ramos, L.L.G. Justino, H.D. Burrows, *Dalton Transactions* 40 (2011) 4374–4383, and references therein.
- [14] See as an example M.V. Kirillova, M.L. Kuznetsov, V.B. Romakh, L.S. Shul’pina, J.J.R. Fraústo da Silva, A.J.L. Pombeiro, G.B. Shul’pin., *Journal of Catalysis* 267 (2009) 140–167.
- [15] D.C. Crans, J.J. Smee, E. Gaidamauskas, L. Yang, *Chemical Reviews* 104 (2004) 849–902.
- [16] J.A.L. da Silva, J.J.R. Fraústo da Silva, A.J.L. Pombeiro, *Coordination Chemistry Reviews* 255 (2011) 2232–2248.
- [17] C. Bolm, *Coordination Chemistry Reviews* 237 (2003) 245–256.
- [18] E. Wojaczyska, J. Wojaczyski, *Chemical Reviews* 110 (2010) 4303–4356.
- [19] J. Gätjens, B. Meier, Y. Adach, H. Sakurai, D. Rehder, *European Journal of Inorganic Chemistry* (2006) 3575–3585.
- [20] C. Song, *Catalysis Today* 86 (2003) 211–263.
- [21] P.S. Kulkarni, C.A.M. Afonso, *Green Chemistry* 12 (2010) 1139–1149.
- [22] P.G. Cozzi, *Chemical Society Reviews* 33 (2004) 410–421.
- [23] A. Zulauf, M. Mellah, X. Hong, E. Schulz, *Dalton Transactions* 39 (2010) 6911–6935.
- [24] P. Adão, M.R. Maurya, U. Kumar, F. Aveçilla, R.T. Henriques, M.L. Kuznetsov, J. Costa Pessoa, I. Correia, *Pure and Applied Chemistry* 81 (2009) 1279–1296.
- [25] V. Conte, F. Fabbianesi, B. Floris, P. Galloni, D. Sordi, I.W.C.E. Arends, M. Bonchio, D. Rehder, D. Bogdal, *Pure and Applied Chemistry* 81 (2009) 1265–1277.
- [26] M. Bonchio, V. Conte, F. Di Furia, G. Modena, S. Moro, J.O. Edwards, *Inorganic Chemistry* 33 (1994) 1631–1637.
- [27] C.P. Horwitz, P.J. Winslow, J.T. Warden, C.A. Lisek, *Inorganic Chemistry* 32 (1993) 82–88.
- [28] N.F. Choudhary, N.G. Connelly, P.B. Hitchcock, G.J. Leigh, *Journal of the Chemical Society, Dalton Transactions* (1999) 4437–4446.
- [29] M.P. Webereski Jr., C.C. McLauchlan, C.G. Hamaker, *Polyhedron* 25 (2006) 119–123.
- [30] A.L. Singer, D.A. Atwood, *Inorganica Chimica Acta* 277 (1998) 157–162.
- [31] C.J. Chang, J.A. Labinger, H.B. Gray, *Inorganic Chemistry* 36 (1997) 5927–5930.
- [32] J.A. Bonadies, C.J. Carrano, *Journal of the American Chemical Society* 108 (1986) 4088–4095.
- [33] M. Salavati-Niasari, A. Badiei, K. Saberyan, *Chemical Engineering Journal* 173 (2011) 651–658.
- [34] E. Tsuchida, K. Yamamoto, K. Oyaizu, N. Iwasaki, F.C. Anson, *Inorganic Chemistry* 33 (1994) 1056–1063.
- [35] T. Ben, I. Zid, A. Keheder, Ghorbel, *Reaction Kinetics Mechanisms* 100 (2010) 131–143.
- [36] J. Zhao, W. Wang, Y. Zhang, *Journal of Inorganic and Organometallic Polymers* 18 (2008) 441–447.
- [37] A. Coletti, C.J. Whiteoak, V. Conte, A.W. Kleij, *ChemCatChem* 4 (2012), <http://dx.doi.org/10.1002/cctc.201100398>.
- [38] M.J. Frisch, G.W. Trucks, H.B. Schlegel, G.E. Scuseria, M.A. Rob, J.R. Cheeseman, J.A. Montgomery Jr., T. Vreven, K.N. Kudin, J.C. Burant, J.M. Millam, S.S. Iyengar, J. Tomasi, V. Barone, B. Mennucci, M. Cossi, G. Scalmani, N. Rega, G.A. Petersson, H. Nakatsuji, M. Hada, M. Ehara, K. Toyota, R. Fukuda, J. Hasegawa, M. Ishida, T. Nakajima, Y. Honda, O. Kitao, H. Nakai, M. Klene, X. Li, J.E. Knox, H.P. Hratchian, J.B. Cross, V. Bakken, C. Adamo, J. Jaramillo, R. Gomperts, R.E. Stratmann, O. Yazyev, A.J. Austin, R. Cammi, C. Pomelli, J.W. Ochterski, P.Y. Ayala, K. Morokuma, G.A. Voth, P. Salvador, J.J. Dannenberg, V.G. Zakrzewski, S. Dapprich, A.D. Daniels, M.C. Strain, O. Farkas, D.K. Malick, A.D. Rabuck, K. Raghavachari, J.B. Foresman, J.V. Ortiz, Q. Cui, A.G. Baboul, S. Clifford, J. Cioslowski, B.B. Stefanov, G. Liu, A. Liashenko, P. Piskorz, I. Komaromi, R.L. Martin, D.J. Fox, T. Keith, M.A. Al-Laham, C.Y. Peng, A. Nanayakkara, M. Challacombe, P.M.W. Gill, B. Johnson, W. Chen, M.W. Wong, C. Gonzalez, J.A. Pople, *Gaussian 03*, Gaussian, Inc., Wallingford, CT, 2003.
- [39] A.D. Becke, *Journal of Chemical Physics* 98 (1993) 5648–5652.
- [40] C. Lee, W. Yang, R.G. Parr, *Physical Review B-Condensed Matter Material Physics* 37 (1988) 785–789.
- [41] Spartan’08 Wavefunction, Inc. Irvine, CA.
- [42] L.P. Hammett, *Physical Organic Chemistry*, 2nd ed., McGraw-Hill, New York, 1970, p. 367.
- [43] O. Bortolini, V. Conte, *Journal of Inorganic Biochemistry* 99 (2005) 1549–1557.
- [44] M. Časný, D. Rehder, *Dalton Transactions* (2004) 839–846, and refs. cited therein.
- [45] G. Zampella, P. Fantucci, V.L. Pecoraro, L. De Gioia, *Journal of the American Chemical Society* 127 (2005) 953–960.
- [46] C.J. Schneider, G. Zampella, C. Greco, V.L. Pecoraro, L. De Gioia, *European Journal of Inorganic Chemistry* (2007) 515–523.
- [47] In Ref. [43], trigonal bipyramidal vanadium complexes are studied where the protonated oxygen is found at binding distances of 2.03–2.08 Å from the vanadium centre. The different results obtained for salophen and salen systems, where that oxygen is located at larger distances, may be ascribed to the their octahedral structure, which hampers the binding of a further coordinating atom.
- [48] F. Ding, J.M. Smith, H. Wang, *Journal of Organic Chemistry* 74 (2009) 2679–2691.

- [49] C.J. Schneider, J.E. Penner-Hahn, V.L. Pecoraro, *Journal of the American Chemical Society* 130 (2008) 2712–2713.
- [50] R.R. Everett, J.R. Kanofsky, A. Butler, *Journal of Biological Chemistry* 265 (1990) 4908–4914.
- [51] J.W.P.M. Van Schijndel, P. Barnett, J. Roelse, E.G.M. Vollenbroek, R. Wever, *European Journal of Biochemistry* 225 (1994) 151–157.
- [52] P. Adão, J. Costa Pessoa, R.T. Henriques, M.L. Kuznetsov, F. Avecilla, M.R. Maurya, U. Kumar, I. Correia, *Inorganic Chemistry* 48 (2009) 3542–3561.
- [53] I.V. Yudanov, P. Gisdakis, C. Di Valentin, N. Rösch, *European Journal of Inorganic Chemistry* (1999) 2135–2145.
- [54] E. Kühn, A.M. Santos, R.W. Rocks, E. Herdweck, W. Scherer, P. Gisdakis, I.V. Yudanov, C. Di Valentin, N. Rösch, *Chemistry-A European Journal* 5 (1999) 3603–3615.
- [55] F.C. Di Valentin, P. Gisdakis, I.V. Yudanov, N. Rösch, *Journal of Organic Chemistry* 65 (2000) 2996–3004.
- [56] S. Lovat, M. Mba, H.C. Abbenhuis, D. Vogt, C. Zonta, G. Licini, *Inorganic Chemistry* 48 (2009) 4724–4728.